



Formation of titanium phosphate composites during phosphoric acid decomposition of natural sphene

Marina V. Maslova^a, Daniela Rusanova^{b,*}, Valeri Naydenov^c, Oleg N. Antzutkin^b, Lidia G. Gerasimova^a

^a Tananaev Institute of Chemistry and Technology of Rare Elements and Mineral Raw Materials, Kola Science Centre, Russian Academy of Sciences, Fersman st. 26a, Apatity, Murmansk Region 184209, Russia

^b Division of Chemistry, Department of Chemical Engineering and Geosciences, Luleå University of Technology, 97187 Luleå, Sweden

^c SunPine AB, Box 76, 941 22 Piteå, Sweden

ARTICLE INFO

Article history:

Received 8 July 2008

Received in revised form

15 September 2008

Accepted 16 September 2008

Available online 25 September 2008

Keywords:

Sphene

Titanite

Titanium phosphate

Brushite

Cs⁺

Si²⁺

ABSTRACT

Decomposition of mineral sphene, CaTiOSiO₄, by H₃PO₄ is investigated in detail. During the dissolution process, simultaneous calcium leaching and formation of titanium phosphate (TiP) take place. The main product of decomposition is a solid titanium phosphate–silica composite. The XRD, solid-state NMR, IR, TGA, SEM and BET data were used to identify and characterize the composite as a mixture of crystalline Ti(HPO₄)₂·H₂O and silica. When 80% phosphoric acid is used the decomposition degree is higher than 98% and calcium is completely transferred into the liquid phase. Formation of Ti(HPO₄)₂·H₂O proceeds via formation of meta-stable titanium phosphate phases, Ti(H₂PO₄)(PO₄)·2H₂O and Ti(H₂PO₄)(PO₄).

The sorption affinities of TiP composites were examined in relation to caesium and strontium ions. A decrease of H₃PO₄ concentration leads to formation of composites with greater sorption properties. The maximum sorption capacity of TiP is observed when 60% H₃PO₄ is used in sphene decomposition.

The work demonstrates a valuable option within the Ti(HPO₄)₂·H₂O–SiO₂ composite synthesis scheme, to use phosphoric acid flows for isolation of CaHPO₄·2H₂O fertilizer.

© 2008 Elsevier Inc. All rights reserved.

1. Introduction

Sphene (CaTiOSiO₄) also known as titanite is a complex orthosilicate mineral occurring in different geological settings [1]. This mineral is of great interest for both geologists and material scientists due to its specific structural and chemical features. Titanite is one of the most important sources of titanium dioxide [2] and it is shown to be an effective geological medium for immobilization of radioactive wastes [3,4]. Recently, the syntheses of sphene-bioactive ceramics reveal a new direction of its applications [5].

Our days, most of the technologies for processing sphene are based on the hydrometallurgical approach. The key step is CaTiOSiO₄ decomposition, usually achieved via dissolution with different inorganic acids, where the leading factor is isolation of titanium in a form suitable for further use. When sulphuric acid is used (70–90% H₂SO₄) an intermediate solid product containing titanium (IV), CaSO₄ and amorphous silica is isolated:



Titanium (IV) is separated from the cake in a subsequent water treatment. The aqueous solution obtained under these conditions is then concentrated and titanyl sulphate monohydrate (TiOSO₄·H₂O) is isolated via controlled crystallization process. This titanium salt is well known source of titanium [3]. When 30–45% sulphuric acid is used in sphene decomposition, the K_s of TiOSO₄·H₂O is not reached and it is left in the liquid phase. Following this scheme the solution is separated from the solid by-products and forwarded for syntheses of titanium phosphates [6–8]:



It has been shown that nitric acid decomposes sphene in a different manner. In the presence of fluoride ions and 25% HNO₃ sphene is effectively decomposed and calcium ions are isolated as a Ca(NO₃)₂ solution. The solid product obtained is a mixture of amorphous silica and crystalline TiO₂ in the anatase form.



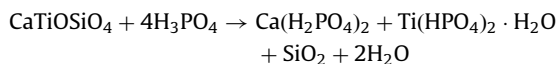
The latter is treated further with 94% sulphuric acid till the soluble titanium salt (TiOSO₄·H₂O) is formed. The titanium-containing aqueous phase allows a concentrated Ti(IV) solution to be obtained which is then used for direct syntheses of titanium oxide pigments as well as for other titanium products [9].

* Corresponding author. Fax: +46 920 49 1199.

E-mail addresses: Daniela.Rusanova@ltu.se, droussanova@hotmail.com (D. Rusanova).

Sphene–acid decomposition schemes often contain complex multistage treatments and require special equipments available (for instance for use of fluorine-containing compounds). Utilization and/or handling of the concomitant acidic flows are also a challenging task.

There are very limited studies on sphene decomposition with H_3PO_4 . To the best of our knowledge, the first attempts to decompose sphene with phosphoric acid are documented in our previous work [10,11]. According to these studies the phosphoric acid decomposition of sphene appears to be somewhat simpler than the aforementioned sulphuric and nitric acids treatments. It also has a great potential when syntheses of different titanium phosphate sorbents is considered.



It is known that most of titanium phosphate materials are obtained from hydrochloric solution of Ti(IV) and H_3PO_4 that is added to the boiling reaction suspension over a long period of time (often a few days) [12–14]. In certain cases, the synthesis follows the sol–gel method [15]. During the sphene decomposition, however, titanium phosphate products are instantly formed.

In this work we show in detail the behavior of sphene during decomposition with phosphoric acid with different concentrations. After thorough characterization of the decompositional products we show that the main product, titanium phosphate–silica composite, can be obtained without implying complex technological steps or special equipments. The present contribution describes the sorption affinities of titanium phosphate–silica composite with respect to caesium and strontium ions, and in addition presents an option for phosphoric acid flows utilization.

2. Experimental section

2.1. Sphene decomposition and titanium phosphate formation. Chemical analyses

Sphene concentrate (fraction $<63\ \mu\text{m}$) with composition (weight %): TiO_2 —37.7, CaO —25.4, SiO_2 —25.4 was used in this study. 40–80% phosphoric acid was utilized in the decomposition processes. Sphene–phosphoric acid amounts in the initial mixtures are listed in Table 1.

The experiment was carried in a reactor equipped with a stirrer and a thermometer, under reflux. In the reactor the calculated amount of phosphoric acid was initially placed and stepwise, under stirring, the corresponding amount of sphene was added. The obtained suspension was heated to the boiling point and at this temperature, and stirring, the mixture was kept for 12 h. During the syntheses on every 2 h samples were taken, the liquid phase was filtrated and both solid and liquid products were analyzed. The chemical composition of the liquid phase was determined using atomic adsorption spectrometer AAS 300 PerkinElmer.

Table 1
Experimental conditions for sphene– H_3PO_4 decomposition process

Concentration of H_3PO_4 (%)	Solid–liquid (g:ml)	(TiO_2+CaO): P_2O_5 (mole, stoichiometric)
80	1:4	1:2.9
70	1:4	1:2.2
60	1:4	1:1.8
50	1:4	1:1.4
40	1:8	1:1.24

The rate of element leaching at these conditions was calculated using the formula [16]:

$$R = \frac{CV}{mt}$$

where R is the leaching rate of element of interest for given time ($\text{mole g}^{-1} \text{s}^{-1}$), C is the concentration of element of interest in the filtrate (mole l^{-1}), V is the filtrate volume (l), m is the mass of sphene (g) and t the time of leaching (sec).

After reaction time (of 12 h) the reaction mixtures were cooled down and solid products isolated (via filtration). The products were then washed with water until pH reached 2.0–3.5 and dried on air at 60°C . The composition of the solid products was analyzed using the standard HF– HNO_3 –HCl method and concentrations of all elements in the resulting solutions were determined using plasma atomic emission spectrometer, ICPE-9000.

2.2. Characterization of decomposition products

The thermogravimetric (TG) and differential thermal analyses (DTA) of samples were carried out in an argon atmosphere using a high-resolution thermogravimetric analyzer (model Netzch STA 409/QMS) in a range of 25– 900°C with a heating rate of $10^\circ\text{C min}^{-1}$.

The powder X-ray diffraction patterns of samples were recorded using a Siemens D 5000 diffractometer with a monochromatic CuK_α radiation ($\lambda = 1.5418\ \text{\AA}$). A scanning rate of $2.4^\circ \text{min}^{-1}$ was used for a 2θ diffraction angle range of 10° – 60° .

To characterize textural properties of titanium phosphate composites, the BET surface areas and the total pore volumes of samples were determined by nitrogen adsorption/desorption method at liquid nitrogen temperature using a surface area analyzer Micrometrics ASAP 2000. Prior to adsorption/desorption measurements all samples were degassed at 373 K for 4 h. This low degassing temperature was chosen to avoid any structural changes in the materials.

The morphologies of samples were studied using a Philips XL 30 scanning electron microscope (SEM) equipped with an LaB_6 emission source. A link ISIS Ge energy dispersive X-ray detector (EDS) attached to the SEM was used to additionally probe the composition of titanium phosphates.

The infrared (IR) spectra were recorded on a Fourier transform IR spectrometer (PerkinElmer FT-IR 2000). A resolution of $4\ \text{cm}^{-1}$ was used with 100 scans averaged to obtain a wavenumber spectrum ranging from 4000 to $370\ \text{cm}^{-1}$. The spectra were recorded in IR-grade KBr phase at room temperature.

The solid-state ^{31}P NMR experiments were recorded at 145.70 MHz on a Varian/Chemagnetics InfinityPlus CMX-360 ($B_0 = 8.46\ \text{T}$) spectrometer. The spectra were acquired using a Varian 4 mm MAS probe and samples were packed in standard ZrO_2 rotors. 10 kHz spinning frequency was used. Single-pulse experiments with proton decoupling were utilized. The 90-pulse width was $5.0\ \mu\text{s}$ and 1 s relaxation delays were used. The total of 256 transients was averaged. All spectra were externally referenced to 85% H_3PO_4 [17]. Deconvolutions of NMR spectra were performed using both Spinsight (a software provided with the spectrometer) and DMfit program [18].

The ^{29}Si NMR spectra were recorded at 71.51 MHz on the same spectrometer. Single-pulse experiments with a proton-decoupled acquisition were used. The spinning frequency of 6 kHz was applied. ^{29}Si 30° pulse width of $1.5\ \mu\text{s}$ and 10 s relaxation delays were employed to avoid saturation of signals. About 9000 numbers of acquisitions were averaged. All spectra were externally referenced to TMS.

The ion-exchange affinity of materials towards Cs^+ and Sr^{2+} cations was probed in a wide pH region using the batch technique.

The 0.05 M solutions of CsCl/SrCl₂ were used and the pH was adjusted using 1 M NaOH or 1M HCl solutions. The 0.5 g of sphene was then added (solid-to-liquid amounts of 1:200) and the suspensions were left to equilibrium for 24 h. The pH of solutions after equilibrium with materials was measured with Orion pH meter 611. Concentrations of metal ions in solutions were determined using AAS-300 atomic absorption spectrometer.

3. Results and discussion

3.1. Sphene decomposition and titanium phosphate formation. Chemical composition

The crystal structure of sphene is shown in Fig. 1. The main structural units are chains of corner-sharing TiO₆ octahedra which are cross-linked by silicate tetrahedra. The SiO₄ tetrahedra share O-atoms with four titanium octahedral groups in three separate chains. Such an arrangement produces [TiOSiO₄]²⁻ skeleton with large cavities where the calcium atoms are enclosed [19]. Precisely, this type of structure would be expected to promote in a certain extend calcium leaching when mineral particles are placed in an appropriate medium. Furthermore, it has been determined that the pH_{pzc} (i.e., the pH at which the surface of solid component in a heterogeneous aqueous system exhibits the neutral net charge) for SiO₂, TiO₂ and CaO are 2.2, 5.5 and 9.9, respectively [20]. This means that in an acidic media the surface calcium sites (>Ca–OH) are expected to be more active than the corresponding titanium and silicate sites (>Ti–OH, >Si–OH) and in a way determining the rate of dissolution of this material. Thus, during sphene acidic decomposition (in particularly when calcium and titanium sites have been already involved in dissolution processes) on the edges of mineral grains an increasing amount of uncompensated negatively charged SiO₄ tetrahedra is expected to built. It is known that under conditions of elevated temperature and acidity the silicate is transformed into silica–SiO₂·H₂O (as is also shown in this study, see further).

Following this model for sphene decomposition we firstly attempted to monitor leaching of calcium into the liquid phase in an H₃PO₄ medium. Fig. 2 shows the degree of Ca leaching when different initial concentrations of phosphoric acid are utilized. Higher concentration of H₃PO₄ governs higher degree of calcium leaching. In the beginning of sphene dissolution the amount of leached calcium rapidly increases with the increase of phosphoric

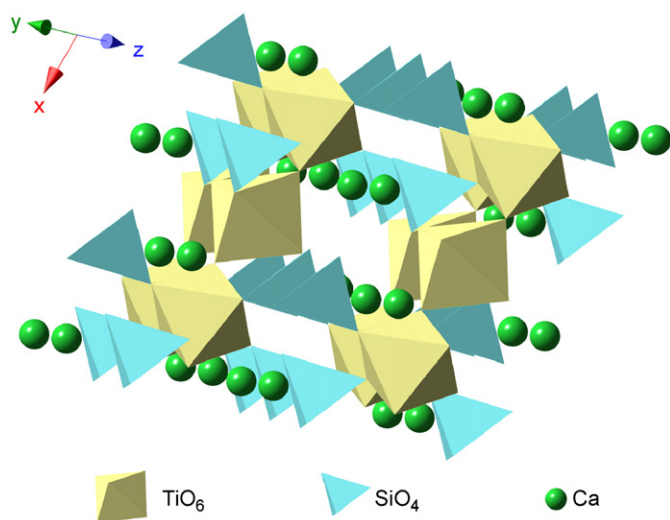


Fig. 1. The crystal structure of sphene (drawn according to data in Ref. [19]).

acid concentration. Such a curve type is consistent with the fact that external diffusion is a dominating mechanism of calcium leaching. As the sphene dissolution proceeds (for instance after the first 2–3 h), the internal diffusion appears to play major role and it is seen that the degree of Ca leaching only gradually increases and is almost constant at the later stages of the reactions (8–12 h).

The rate of calcium leaching/dissolution is also determined by the acid concentration (as seen in Fig. 3). Higher concentration of H₃PO₄ used lead to faster dissolution. After 8 h the rate of calcium dissolution is less than 1×10^{-7} mole g⁻¹ s⁻¹ and practically does not depend on the initial phosphoric acid concentrations.

During the sphene decomposition the calcium leaching process takes place together with a titanium phosphate formation process. These two concomitant processes were considered when the final decomposition products were analyzed. The chemical compositions of final products are listed in Table 2. Titanium found in the solid phase can be in a form of titanium phosphate and/or in a form of CaTiOSiO₄ (i.e., non-dissolved sphene). Thus, the amount of titanium phosphate was calculated based on the amounts of TiO₂ and P₂O₅ found in the solid phase products. Based on the XRD powder pattern analyses (see further), formation of titanium hydrogen phosphate hydrate, Ti(HPO₄)₂·H₂O, where the mole

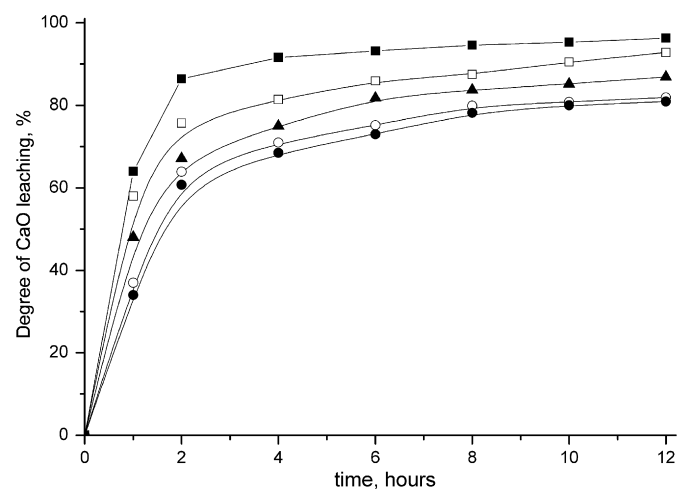


Fig. 2. The degree of Ca leaching (expressed as CaO, %) during sphene decomposition with 80% (■), 70% (□), 60% (▲), 50% (○) and 40% (●) H₃PO₄, respectively. The lines are a guide for the eye.

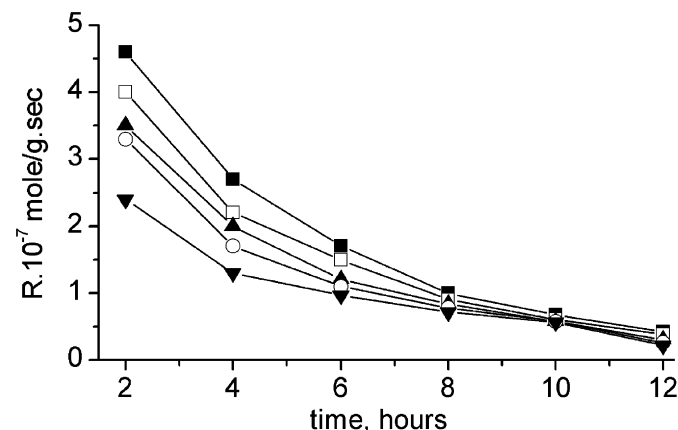


Fig. 3. The rate of Ca leaching during sphene decomposition with 80% (■), 70% (□), 60% (▲), 50% (○) and 40% (●) H₃PO₄, respectively. The lines are a guide for the eye.

Table 2
Chemical composition of products from sphene decomposition

Concentration of H ₃ PO ₄ (%)	Content of solids (mole)				Decomposition (degree)
	TiO ₂	P ₂ O ₅	CaO	SiO ₂	
80	0.265	0.27	0.02	0.28	98.1
70	0.28	0.26	0.04	0.30	92.9
60	0.31	0.24	0.06	0.32	91.2
50	0.34	0.23	0.09	0.33	67.6
40	0.35	0.22	0.09	0.34	62.8

ratio of TiO₂:P₂O₅ is 1:1, was confirmed. Hence, the amount of titanium (by mole) not connected to P₂O₅ is considered as titanium in CaTiOSiO₄. The data in Table 2 show that when 80% H₃PO₄ was used, the degree of sphene decomposition (calculated using the amount of TiO₂ not in the titanium phosphate form) is more than 98% whilst for 40% acid only about 63% decomposes. As mention above, the decrease of acid concentration leads to the decrease of calcium leaching rate. At the same time this is supposed to slow down the expected diffusion drift of titanium ions towards the particle surfaces and hence the simultaneous crystallization of titanium phosphates to be relatively unhurried. In all experiments, the amount of phosphoric acid used was higher than the stoichiometric amount required for binding both calcium and titanium in corresponding phosphates. Despite this fact the degree of sphene decomposition appears to be higher when higher concentration of acid is used. The excess of phosphoric acid is likely to have a major effect on the rate of formation of titanium phosphate [21].

Within the examined conditions of sphene decomposition it was found that a process of Si leaching (8×10^{-3} mole l⁻¹) took place only when 80% phosphoric acid was used. In all other cases conditions for Si leaching were not fulfilled and the SiO₄ tetrahedra were considered to only alter to SiO₂·nH₂O and/or SiO₂ (see discussion on results in Figs. 6 and 11). Formation of an amorphous silica phase occurs as the structure of sphene wrecks during the phosphoric acid's attack. Under these experimental conditions, the silica sites are least active sites (in comparison to calcium and titanium sites) during the sphene dissolution.

3.2. Characterization of decomposition products—titanium phosphate composites

Fig. 4 shows the thermal behavior of two sphene decomposition products obtained after 12 h reaction time using solutions with 80% and 40% H₃PO₄. Both TGA curves show similar gradual weight loss patterns. The first weight loss, 6% for both (equivalent to 0.87 mole of water per formula unit), corresponds to a loss of surface and/or crystal water at temperature up to 250 °C. The second weight loss, 5.8% for both (0.83 mole of H₂O), in the range of 250–580 °C, is attributed to condensation of hydrogen phosphate functional groups. The total weight loss is 11.8% and 13.6% for these products, obtained with 80% and 40% H₃PO₄, respectively. It should be noted here that the use of a less concentrated acid to decompose the sphene somewhat leads to formation of products with a slightly different internal structure. In particular, for the product obtained with 40% H₃PO₄, additional weight loss (of 1.8%) at temperature higher than 600 °C is observed. This can be assigned to a later condensation process that involves silanol groups in the material. These data are in a good agreement with DTA data reported for the thermal behavior of alpha-titanium phosphate, α-TiP (Ti(HPO₄)₂·H₂O) [22,23].

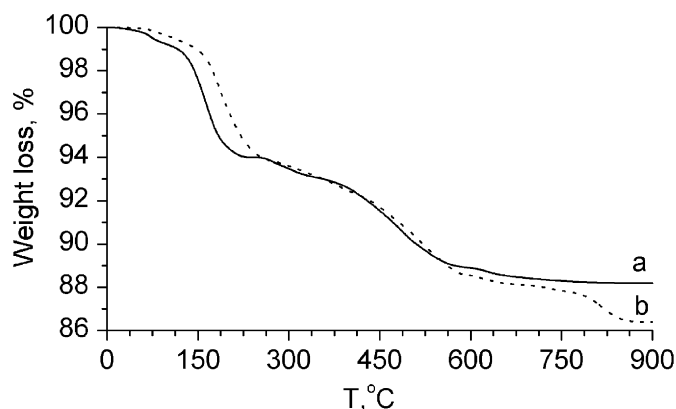


Fig. 4. The TG data for titanium phosphate composites obtained at 12 h decomposition of sphene with 80% (a) and 40% (b) phosphoric acid.

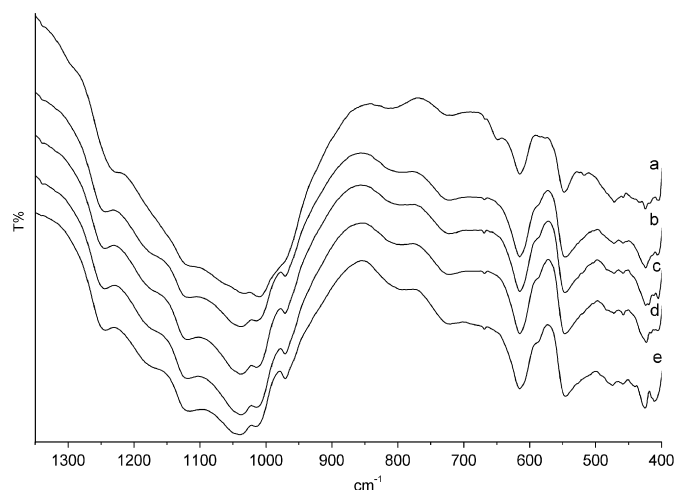


Fig. 5. The IR spectra of sphene–60% H₃PO₄ decomposition products isolated after 2 h (a), 4 h (b), 6 h (c), 8 h (d) and 12 h (e), respectively.

Fig. 5 shows the IR spectra (over the 1400–400 cm⁻¹ region) for decomposition products isolated after different reaction times of sphene treated with 60% H₃PO₄. All spectra have very similar features that appear to be characteristic for the IR spectrum of α-TiP [24,25]. With an increase of decomposition time the bands attributed to the phosphate groups ((PO₃)_{asym} and (PO₃)_{sym} in the region of 1000–1240 cm⁻¹, (PO₃) deformation modes at the 615, 470 and 440 cm⁻¹ and the symmetric mode characterizing P–O–P bridges at around 970 cm⁻¹), become more resolved. This is a strong indication of internal changes in the titanium composite structures. The intensity of band at 548 cm⁻¹ increases with the decrease of sphene content in the composites which shows its relevance to the P–O vibration [26] and not to Ti–O in the octahedral oxygen environment [27]. Differences in the spectrum of the product obtained after 2 h of decomposition are observed in Fig. 5a. The P–OH vibrations at 1249 cm⁻¹ (from HPO₄²⁻) are overlapped with the vibrations at 1231 cm⁻¹ which are characteristics of P–OH in H₂PO₄⁻ groups [28]. The adsorption at 651 cm⁻¹, which is special for O–P–O vibrations in PO₄ groups and the absence of the band at 970 cm⁻¹ (a characteristic of P–O–P in HPO₄ groups) suggest that in this decomposition product along with the α-TiP phase, there is a γ-TiP phase, Ti(H₂PO₄)·(PO₄)·2H₂O, or a mixture of γ-TiP and β-TiP, Ti(H₂PO₄)·(PO₄), phases. The last two phases are known to be

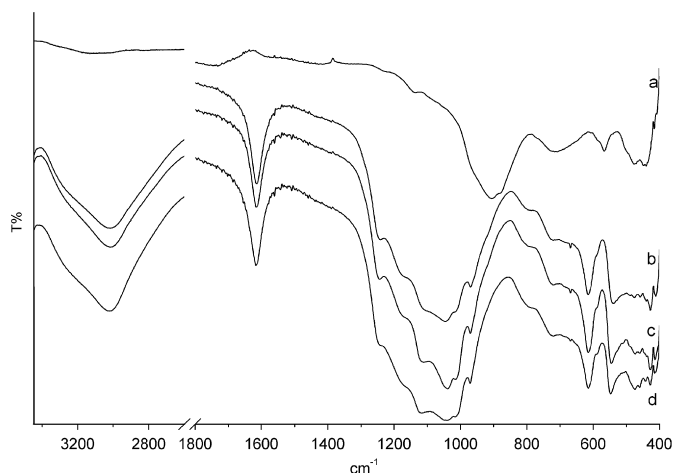


Fig. 6. The IR spectra of sphene (a) and titanium phosphate composites (b–d) isolated after 12 h. The phosphoric acid concentration used was 80% (b), 60% (c) and 40% (d), respectively.

meta-stable at high temperature conditions and easily transform into the α -phase [29].

Fig. 6 shows the IR spectra from products obtained after 12 h sphene decomposition with different concentration of phosphoric acid. It can be seen that despite the differences in H_3PO_4 concentration all decomposition products appeared to be of the α -TiP-type. The main features that differ in these spectra are related to stretching and bending vibrations of the OH groups in the $3560\text{--}1600\text{ cm}^{-1}$ region. This is most likely caused by an increase of silica hydration as far as concentration of acid decreases. Furthermore, for samples where the non-decomposed sphene is almost 40% the characteristic adsorption bands for the mineral are not observed (see Fig. 6d). In particular, the Si–O vibrations of SiO_4 tetrahedra at about 900 cm^{-1} are absent which is a clear indication for changes in Si–O environment in the structure of undissolved sphene particles.

The XRD powder data for products of sphene–phosphoric acid (80–40%) decompositions are displayed in Fig. 7. All data are consistent with formation of a titanium phosphate crystalline phase, $\text{Ti}(\text{HPO}_4)_2 \cdot \text{H}_2\text{O}$ [30] with a first intensive 2θ peak corresponding to $d = 8.6\text{ \AA}$. A decrease of phosphoric acid concentration (used in the sphene decomposition) leads to a gradual decrease of intensities of titanium phosphate reflections. The reflections due to the non-decomposed sphene are more noticeable among the titanium phosphate ones in the cases of 40–60% acid used. For the sake of simplicity selected sphene reflections are denoted with an asterisk throughout the powder patterns in the figure. It should be noted that the most intensive sphene reflection (about $34.5\ 2\theta$) is not denoted in the figure due to the possible overlap with titanium phosphate reflections in this 2θ region. The kinetics of decomposition (shown in Fig. 8) shows that when 80% H_3PO_4 was in use already after the first 2 h the main phase formed is the aforementioned α -TiP (similarly as in Fig. 7 selected sphene reflection are denoted with an asterisk). For the same reaction time and 60% H_3PO_4 employed, the obtained solid product is a mixture of α -, γ -TiP (and possibly β -TiP) [31] phases of poor crystallinity as well as non-decomposed sphene. Interestingly, when 40% phosphoric acid was used, after 2 h the main crystalline phase appears to be somewhat altered non-decomposed sphene particles (compare Figs. 7a and 8e). Common features for the powder diffractograms of products obtained after 2 h, using 40 and 60% H_3PO_4 , that makes them very complex for assessment, lead to suggestion for a possible existence of $\text{Ti}(\text{HPO}_4)_2 \cdot 2\text{H}_2\text{O}$ along with the sphene and $\text{Ti}(\text{HPO}_4)_2 \cdot \text{H}_2\text{O}$.

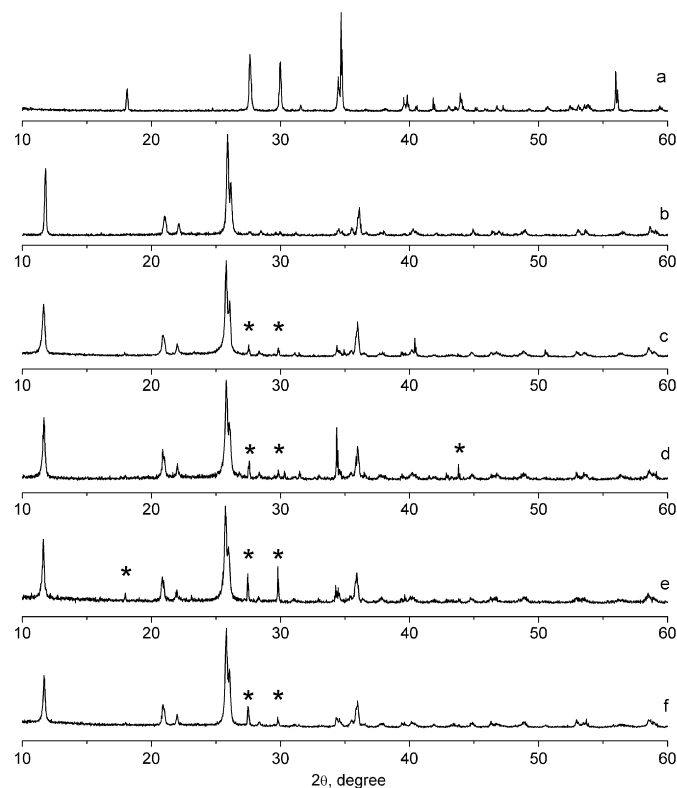


Fig. 7. The XRD powder patterns of sphene (a) and titanium phosphate composites (b–f) isolated after 12 h. The phosphoric acid concentration used was 80% (b), 70% (c), 60% (d), 50% (e) and 40% (f), respectively. In powder patterns (c), (d), (e) and (f), the reflections due to presence of sphene phase are denoted with an asterisk.

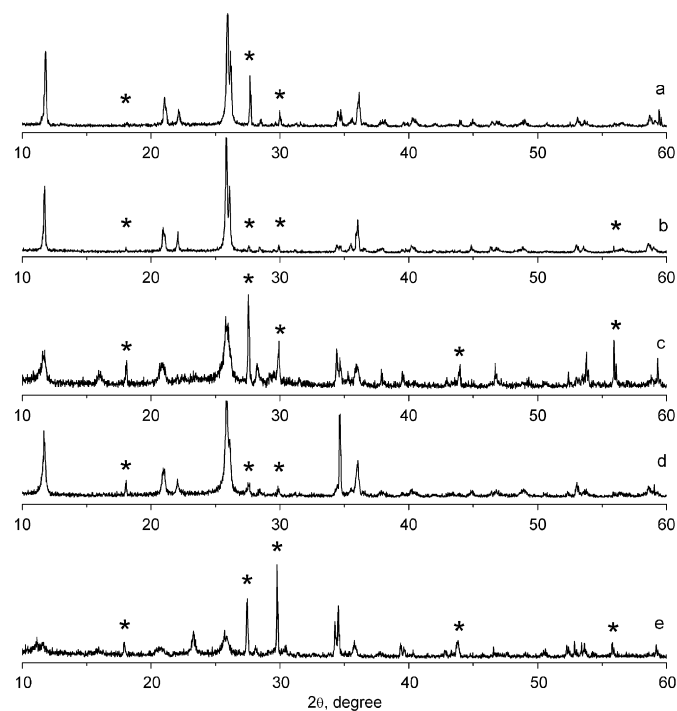


Fig. 8. The XRD powder patterns of sphene decomposition products. The phosphoric acid concentration used was 80% (a, b), 60% (c, d) and 40% (e). Products were isolated after 2 h (a, c and e) and 4 h (b, d), respectively. The reflections due to presence of sphene phase are denoted with an asterisk.

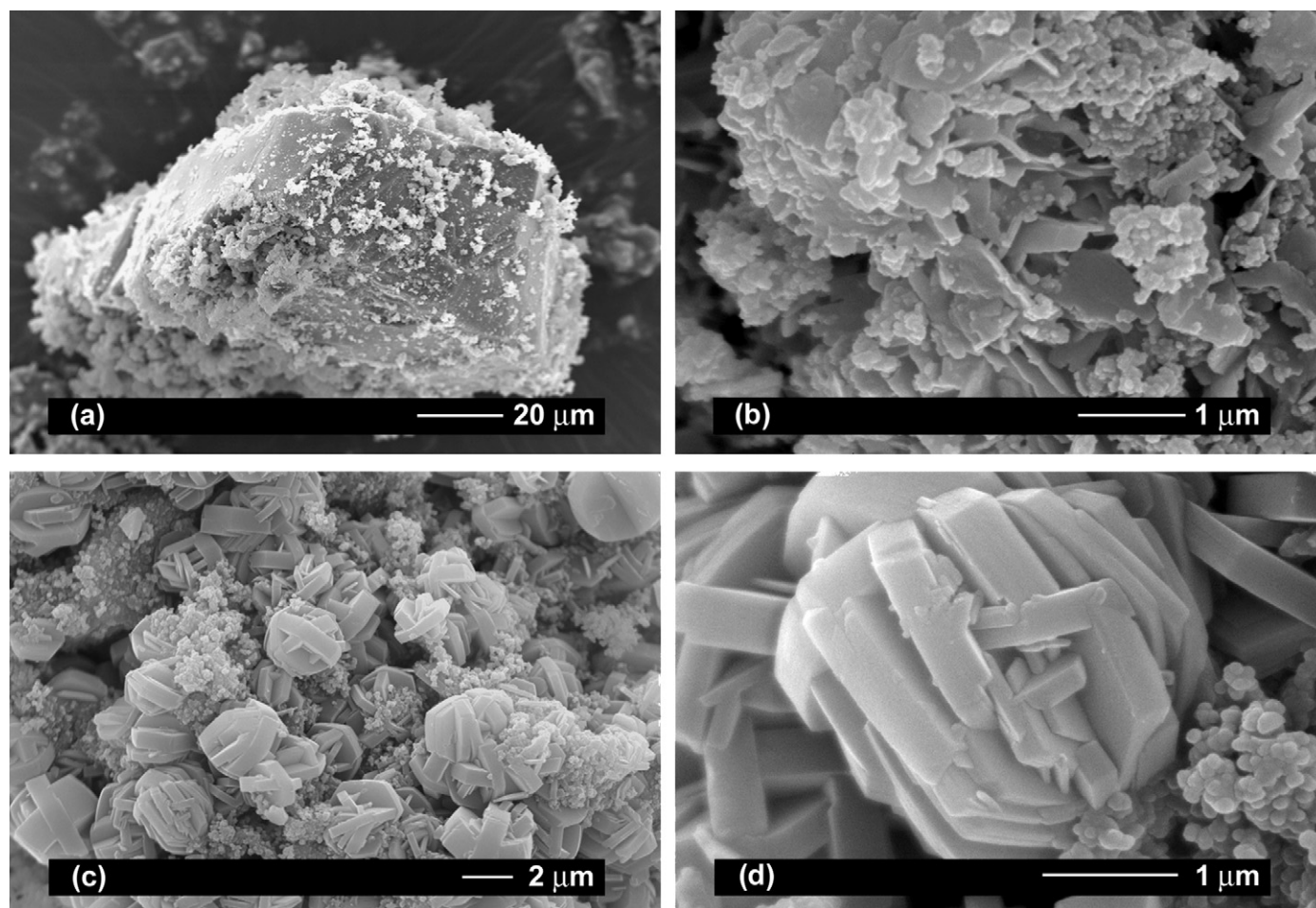


Fig. 9. The SEM images of sphene (a), titanium phosphate composites isolated after 2 h, 40% H_3PO_4 (b) and titanium phosphate composites after 12 h, 80% H_3PO_4 at different magnification (c, d).

However, the reflections characteristic for the titanium phosphate di-hydrate are of very low intensity. (Detailed diffractograms along with results from the XRD powder patterns database can be found in the Supporting information appended to this article.)

SEM images of initial sphene and sphene decomposition products are shown in Fig. 9. It is seen how in an early stage flake-like structures of titanium phosphate are formed along with small spherical silica agglomerates. The final titanium phosphate composites contain ball-like structures of titanium phosphate (with diameter of ca 2 μm), randomly distributed in a silica matrix.

The ^{31}P MAS NMR spectrum of titanium phosphate composite obtained after 12 h process and 80% H_3PO_4 is shown in Fig. 10a. A single, relatively narrow phosphorus resonance peak at -18.4 ppm is observed. The same ^{31}P -isotropic chemical shift was recorded in the ^{31}P MAS NMR spectra of all titanium phosphate composites obtained after 4–12 h decomposition of sphene in the whole concentration range of phosphoric acid (40–80%). It has been reported that the $\delta_{\text{iso}}(^{31}\text{P})$ for the P-sites in the crystalline α - TiP is -18.5 ppm [32,33]. Therefore, it can be unambiguously concluded that the titanium phosphate composites obtained at the aforementioned conditions only contain P-sites in a $\text{Ti}(\text{HPO}_4)_2 \cdot \text{H}_2\text{O}$ environment. In Fig. 10b, the ^{31}P MAS NMR spectrum of titanium phosphate composite obtained after a 2 h process with 40% phosphoric acid used is displayed. A similar spectrum was also obtained for the composite formed in a 2 h

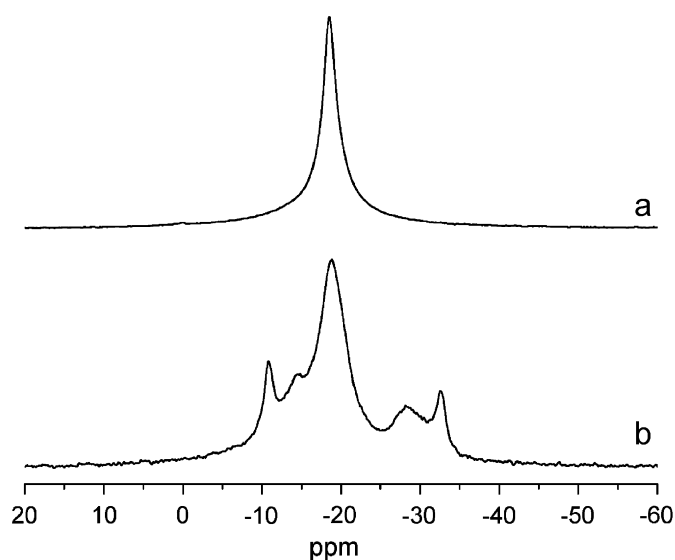


Fig. 10. The ^{31}P NMR spectra of titanium phosphate composites obtained after (a) 12 h, 80% H_3PO_4 and (b) 2 h, 40% H_3PO_4 .

process with 60% H_3PO_4 . The composites obtained in 2 h processes with higher than 60% phosphoric acid show ^{31}P MAS NMR spectra that are similar to the spectrum in Fig. 10a.

A detailed look at the spectrum in Fig. 10b reveals an overlap of five ^{31}P -resonances centered at -10.8 , -14.4 , -18.4 , -28.2 and -32.6 ppm, respectively. The phosphorus isotropic chemical shift at -18.4 ppm as described above appears to be a characteristic for phosphorus in the α -TiP, while the δ_{iso} (^{31}P) at -10.8 and -32.6 ppm are associated with the phosphorus sites in H_2PO_4^- and PO_4 local environments in the γ -TiP, $\text{Ti}(\text{H}_2\text{PO}_4) \cdot (\text{PO}_4) \cdot 2\text{H}_2\text{O}$ [32,33]. The P-sites at -14.4 and at -28.2 ppm have not yet been assigned to particular P-sites in crystalline titanium phosphates. It has been reported, however, that on some occasions the γ -TiP phase co-exists with the less stable phase, $\text{Ti}(\text{H}_2\text{PO}_4) \cdot (\text{PO}_4)$ [29]. Therefore it could be suggested that these phosphorus sites belong to the anhydrous β -type where two crystallographically different phosphorus sites have been determined [34]. A possibility, which should not be excluded in the interpretation of the spectrum, is that these P-sites (at -14.4 and -28.2 ppm) may not be related to phosphate coordination in β -TiP-phase but are simply a result of different Ti–O–P bond distances and bond angles somewhat formed between the different species at these experimental conditions. Deconvolution of the spectrum shows that the amount of α -TiP formed already at these conditions is higher than 50%.

In short, the ^{31}P MAS NMR data clearly show that formation of α -TiP composites proceeds via formation of γ -TiP (and possibly β -TiP) and the latter appeared to be meta-stable under these conditions. The mixture of these products is maintained only during the first 2–3 h of sphene decomposition process with 40–60% phosphoric acid. In all other decomposition conditions only the α -TiP composite is formed.

The ^{29}Si NMR spectra of sphene and the titanium phosphate composites are shown in Fig. 11. The Si-sites with isotropic chemical shift at about -80 ppm corresponds to the silicate sites in sphene [35]. In Fig. 11b it can be seen that together with the sites from non-decomposed sphene another type of Si-species is built when decomposition is performed with 40% acid, for 12 h. The isotropic silicon peak at about -112 ppm is rather broad and is characterized with a shoulder at about -102 ppm. A similar ^{29}Si NMR spectrum but with a less resolved shoulder is observed when decomposition was done with 80% acid for 2 h (Fig. 11c). It has been reported that silica fume exhibits a broad ^{29}Si NMR resonance at -111.5 ppm, which belong to the classic Q^4 Si type ($4\text{Si}, 0\text{Ti}$) that is a characteristic of fully polymerized silica species [36,37]. Therefore, here it can be concluded that during the decomposition of sphene the silicate sites undergo a transformation that leads to formation of SiO_2 entities. The species at -102 ppm are of the corresponding Q^3 type and are related to the presence of silanol groups [37]. Due to less amount of water present in the system they are less pronounced when 80% acid is used in the decomposition. As it can be seen in Fig. 11d when 80% H_3PO_4 is used, for 12 h period of time, almost entire amount of silicate in sphene is transformed into a separate silica phase.

The IR, XRD, SEM and solid-state NMR data are all in a good agreement and show that during the process of sphene decomposition with phosphoric acid, a crystalline α -titanium phosphate-silica composite is simultaneously built.

3.3. Ion-exchange properties of titanium phosphate composites

The ion-exchange affinity of titanium phosphate composites towards Cs^+ and Sr^{2+} at different pH conditions was probed. The experimental curves for cations uptake at different pH-values are shown in Fig. 12. Taking into account the amount of titanium phosphate within the composites, the chemical formula of α -TiP and the assumption that all protons are exchangeable, the theoretical ion-exchange capacity of the products was

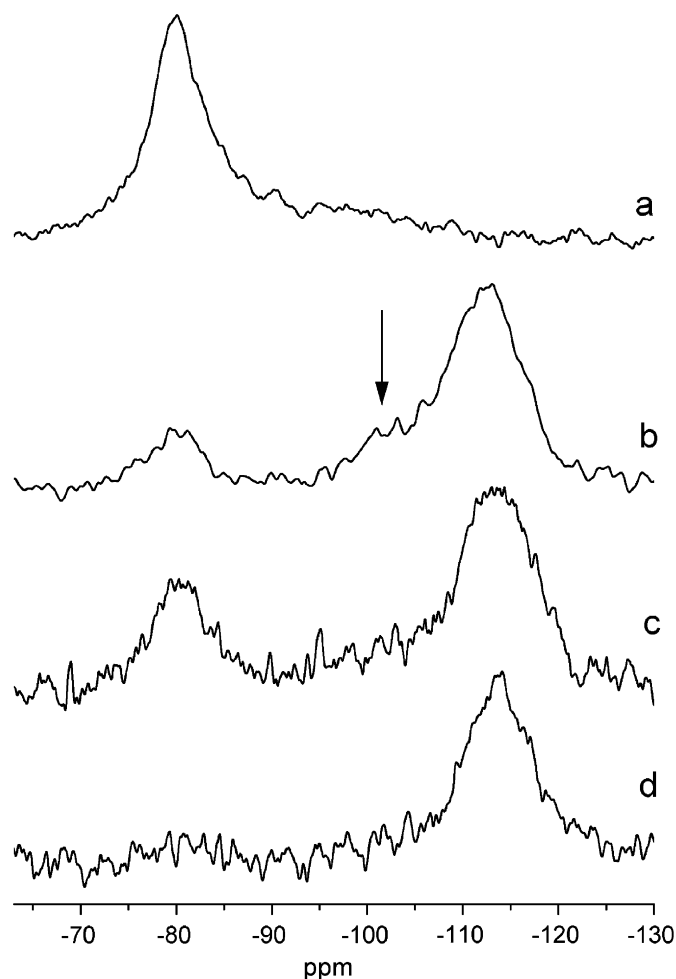


Fig. 11. The ^{29}Si NMR spectra of (a) sphene and sphene-phosphoric acid decomposition products obtained at (b) 40% H_3PO_4 , 12 h; (c) 80% H_3PO_4 , 2 h; (d) 80% H_3PO_4 , 12 h. The arrow indicates the shoulder at -102 ppm.

calculated to be in the range from 4.87 to 7.60 meq g^{-1} . The titanium phosphate composites start to exchange Cs^+ ions at pH 2 (see Fig. 12a) and yet metal uptake is insignificant even at pH 10. The Cs^+ maximum uptake is 1.62 meq g^{-1} (or 23%) for the composite obtained with 60% H_3PO_4 . The titanium phosphate composite formed with 40% H_3PO_4 contains up to 40% sphene, which is likely to be the reason for the lower sorption activity detected. At the same time the sorption properties of these two composites are considerably higher than the properties of product obtained with 80% H_3PO_4 . As seen from the XRD data and the porous characteristics of the materials (listed in Table 3), stronger synthesis conditions lead to formation of more crystalline material that is expected to have a higher rigidity that restrains insertion of large cations. Lowering concentration of phosphoric acid for decomposition of sphene somewhat promotes formation of a more porous structure which can be correlated with higher sorption activity. Experimental curves showing the Sr^{2+} uptake at different pH conditions are shown in Fig. 12b. For the titanium phosphate composites obtained with 60% H_3PO_4 the strontium uptake is 0.2 – 0.4 meq g^{-1} in an acidic medium and reaches its maximum (1.2 meq g^{-1}) at pH 9. The low sorption activity toward this cation is most likely due to geometrical incompatibilities between the ion-exchange sites in the TiP composite and the size of cation. The strontium ion is characterized with larger hydration shell than the caesium hydrated ion [38] and therefore appears to be too large to freely diffuse into the solid exchanger. The

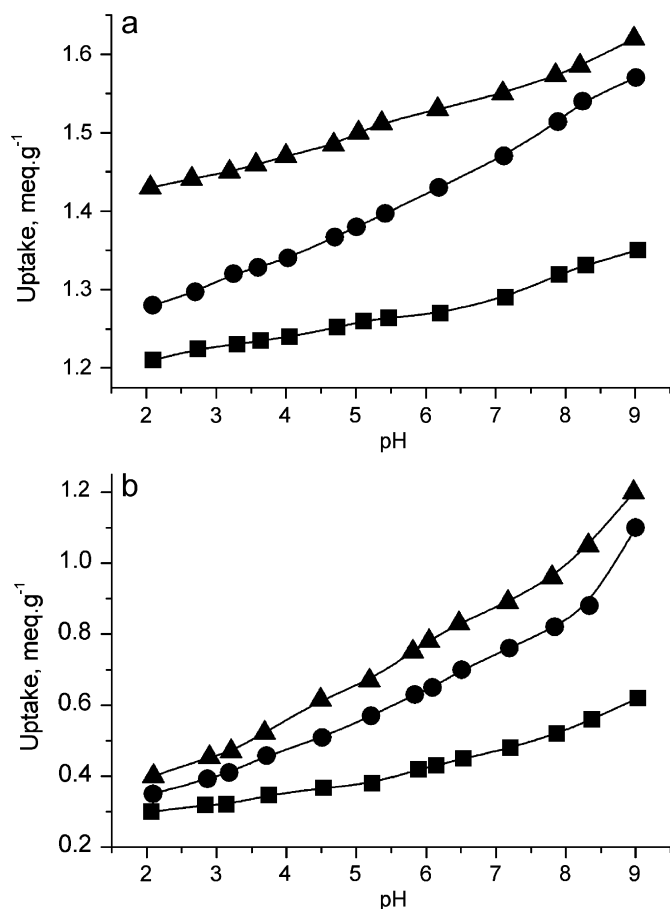


Fig. 12. The Cs^+ (a) and Sr^{2+} (b) uptake by titanium phosphate composites obtained under decomposition of sphene with 40% (●), 60% (▲) and 80% (■) phosphoric acid. The lines are a guide for the eye.

Table 3

BET-surface area, total pore volume and mean pore diameter data for materials obtained at 12 h decomposition of sphene with 40%, 60% and 80% phosphoric acid

Sample (%)	Surface area ($\text{m}^2 \text{g}^{-1}$)	Total pore volume $\times 10^3$ ($\text{cm}^3 \text{g}^{-1}$)	Mean pore diameter (nm)
40	17.29 ± 0.03	72.38	16.75
60	4.91 ± 0.01	28.21	22.98
80	1.67 ± 0.02	7.01	16.79
Sphene	1.82 ± 0.01	5.72	12.55

exchange properties of TiP towards strontium ions show a similar trend that was observed with respect to the caesium ions, namely, the highest sorption affinity is found for composites formed with 60% H_3PO_4 acid, following by those obtained with 40% and finally the products gathered when 80% acid was used. Such a trend is somewhat in agreement with the textural characteristics of composites (listed in Table 3). Products of decomposition with 60% acid have largest mean pore diameter which is expected to play an important role in ion-exchange processes. Moreover, analyses of ion-exchange capacities of titanium phosphate composites show that these materials possess sorption behavior that is similar to the exchange affinity of titanium silicates [39,40] and therefore have a great potential as solid ion-exchangers.

Additionally, the solutions/filtrates from the sorption experiments were analyzed for Ti and P contents in order to monitor the hydrolytic stability of the composites. The process of hydrolysis, expressed in a substitution of hydroxy-phosphate groups with hydroxyl groups, was observed only for the materials obtained with 40–50% H_3PO_4 . When higher concentration of phosphoric acid was used the phosphorus hydrolysis was negligible. The titanium hydrolysis, monitored by the concentration of Ti(IV) in the solutions, was also found to be negligible (0.01–0.03%) and decreases with an increase of pH-value.

It is known that with an increase of contact time between the sorbent and aqueous solution, the rate of hydrolysis decreases. To compare the hydrolytic stability of different titanium phosphate ion-exchangers at different experimental acid/base media the mean hydrolysis rate was calculated using the following equation [41]:

$$v = C_e[V/m]\tau$$

where C_e is the equilibrium concentration of phosphate ions in solution (calculated as P_2O_5 (mg l^{-1})), V is the volume of solution (l), m is the exchanger mass (g) and τ the contact time (h) between the materials and the aqueous solutions.

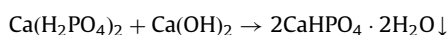
The mean hydrolysis rate of titanium phosphate products at pH 3–6 was found to be 4.28×10^{-8} and $9.76 \times 10^{-7} \text{ mg g}^{-1} \text{ h}^{-1}$ for compounds obtained with 50 and 40% H_3PO_4 , respectively. For composites formed with a higher concentration of phosphoric acid the hydrolysis rate was very low and practically undetectable.

3.4. Utilization of calcium-containing phosphoric acid flows

In the processes of sphene decomposition and washing of final products (during the washing of final decomposition products, dissolution of calcium-containing phases takes place) an acidic flow, containing different amounts of phosphoric acid and calcium ions, is generated. In particular, when 70–80% H_3PO_4 is used, calcium is concentrated in the liquid phase (due to the concomitant leaching process) and when the solubility product of $\text{Ca}(\text{H}_2\text{PO}_4)_2 \cdot \text{H}_2\text{O}$ is reached the latter precipitates in the system. A decrease of acid concentration causes less amount of solid $\text{Ca}(\text{H}_2\text{PO}_4)_2 \cdot \text{H}_2\text{O}$ to be formed and hence the amount of calcium in the liquid phase is higher. When 40% H_3PO_4 is used all calcium is practically in the liquid phase until the end of the process. Depending on the decomposition conditions it is found that the phosphoric acid flow contains 100–800 g l^{-1} P_2O_5 and 20–60 g l^{-1} CaO. According to the solubility diagram of the system $\text{CaO}-\text{P}_2\text{O}_5-\text{H}_2\text{O}$ [42] at high concentration of P_2O_5 (57%) a calcium dihydrogenphosphate, $\text{Ca}(\text{H}_2\text{PO}_4)_2$ is formed. A decrease of this concentration governs formation of calcium hydrogenphosphate, $\text{CaHPO}_4 \cdot 2\text{H}_2\text{O}$.

In this study we show how the phosphoric acid flows from the sphene decomposition and washing procedures can be utilized and another industrially important product isolated.

For this purpose a $\text{CaO}-\text{P}_2\text{O}_5-\text{H}_2\text{O}$ mixture containing 500–650 g l^{-1} P_2O_5 was step-wise neutralized with slaked lime (10% CaO), when the ratio $\text{CaO}:\text{P}_2\text{O}_5$ was 0.79. The precipitation occurs according to the following equations:



To avoid co-precipitation of $\text{Ca}_3(\text{PO}_4)_2$ the mixture was constantly stirred. The crystallization started at pH 3.0–3.2 and was completed at pH 6.3. Duration time was 1.5–2 h and after it the precipitation was filtered and water-washed. The XRD pattern of the solid obtained at these conditions is consistent with the XRD pattern of brushite (see Fig. 13). The obtained calcium salt,

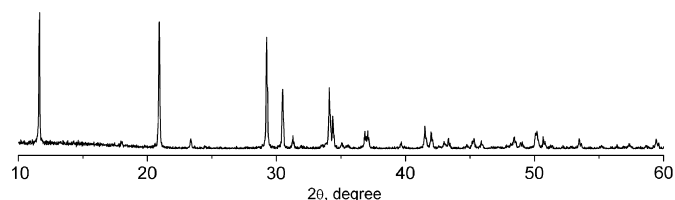


Fig. 13. The XRD powder pattern of the solid product isolated from calcium-containing H_3PO_4 flows.

$\text{CaHPO}_4 \cdot 2\text{H}_2\text{O}$, is in the form of brushite– a well-known fertilizer with high content of an active component (the phosphorus). It should be noted that if the neutralization is carried on with lime the final product is anhydrous CaHPO_4 , which does not have the capacity to support plant growth.

4. Conclusions

The sphene– H_3PO_4 decomposition process is accompanied with calcium leaching and titanium phosphate formation processes. The decomposition product is a solid titanium phosphate–silica composite. It was observed that with a decrease of phosphoric acid concentration the hydration of silica increases whilst the rigidity of titanium phosphate structures decreases.

An increase of H_3PO_4 concentration leads to an increase of decomposition degree and when 80% acid is used, it is higher than 98%. The kinetics of decomposition shows that using 80% acid results, already after 2 h, in formation of α -TiP, $\text{Ti}(\text{HPO}_4)_2 \cdot \text{H}_2\text{O}$, whilst using 40% phosphoric acid for the same time results mainly in altering the initial sphene particles. It is revealed that formation of $\text{Ti}(\text{HPO}_4)_2 \cdot \text{H}_2\text{O}$ proceeds via formation of meta-stable titanium phosphate phases, $\text{Ti}(\text{H}_2\text{PO}_4)(\text{PO}_4)$ and $\text{Ti}(\text{H}_2\text{PO}_4)(\text{PO}_4) \cdot 2\text{H}_2\text{O}$, which are only maintained in first two hours of sphene decomposition with 60–40% H_3PO_4 .

The sorption properties of titanium phosphate composites were probed towards caesium and strontium ions at different pH conditions. It was observed that harder synthesis conditions lead to formation of materials with higher stiffness that hinders inclusion of large cations. A decrease of the phosphoric acid concentration promotes formation of more porous structures which possess higher sorption affinity. The maximum sorption capacity was observed for TiP-products obtained during sphene decomposition with 60% H_3PO_4 .

A possibility to use further the phosphoric acid flows by isolating $\text{CaHPO}_4 \cdot 2\text{H}_2\text{O}$ fertilizer is demonstrated. This shows an opportunity the sphene– H_3PO_4 decomposition process to be technologically designed in such a way that all steps are interconnected and all by-products utilized.

Acknowledgments

M. Maslova thanks The Swedish Institute for the partial financial support of this work. The foundation to the memory of J.C. and Seth. M. Kempe is acknowledged for Grants (JCK-2003, JCK-2007) used for updating Varian/Chemagnetics CMX-360 NMR spectrometer.

Appendix A. Supporting information

Detailed diffractograms for Figs. 7, 8 and 13 along with results from the XRD powder patterns database can be found in the online version at doi:10.1016/j.jssc.2008.09.007.

References

- [1] W.A. Deer, R.A. Howie, J. Zussman, *Orthosilicates: Sphene (Titanite), Rock-Forming Minerals*, vol. 1A, Longman, London, 1977, pp. 443–466.
- [2] D.L. Motov, G.K. Maksimova, *Titanite and its Chemical Processing for Production of Titanium Pigments*, Nauka, Leningrad, 1983.
- [3] M. Muthuraman, N.A. Dhas, K.C. Patil, *Bull. Mater. Sci.* 17 (1994) 977.
- [4] M. Gascoyne, *Appl. Geochem.* 1 (1986) 199.
- [5] C. Wu, Y. Ramaswamy, A. Soeparto, H. Zreiqat, *J. Biomed. Mater. Res. Part B* 86A (2008) 402.
- [6] I.V. Lazareva, L.G. Gerasimova, R.F. Okhrimenko, M.V. Maslova, *Russ. J. Appl. Chem.* 79 (2006) 16.
- [7] L.G. Gerasimova, M.V. Maslova, N.M. Zhdanova, R.F. Okhrimenko, *Russ. J. Appl. Chem.* 74 (2001) 1786.
- [8] M.V. Maslova, L.G. Gerasimova, R.F. Okhrimenko, A.S. Chugunov, *Russ. J. Appl. Chem.* 79 (2006) 1793.
- [9] E.P. Lokshin, T.A. Sedneva, I.A. Tikhomirova, *Russ. J. Appl. Chem.* 77 (2004) 1041.
- [10] L.G. Gerasimova, M.V. Maslova, V.A. Matveev, *Sphene concentrate processing method*, Patent number: RU2235685 C, 2004.
- [11] M.V. Maslova, L.G. Gerasimova, *Russ. J. Appl. Chem.* 79 (2006) 1565.
- [12] A. Clearfield, J.A. Stynes, *J. Inorg. Nucl. Chem.* 26 (1964) 117.
- [13] G. Alberti, P. Cardini-Galli, U. Constantino, E. Torracca, *J. Inorg. Nucl. Chem.* 29 (1967) 571.
- [14] A. Nilchi, M.G. Maragheh, A. Khanchi, et al., *J. Radioanal. Nucl. Chem.* 261 (2004) 393.
- [15] A.I. Bortun, L.N. Bortun, A. Clearfield, S.A. Khainakov, et al., *Solv. Extr. Ion Exch.* 5 (1997) 515.
- [16] B.E. Kalinowski, P. Schweda, *Geochem. Cosmochim. Acta* 60 (1996) 367.
- [17] K. Karaghiosoff, *Encyclopedia of Nuclear Magnetic Resonance*, vol. 6, Wiley, New York, 1996, p. 3612.
- [18] D. Massiot, F. Fayon, M. Capron, et al., *Magn. Reson. Chem.* 40 (2000) 70 DMfit program. Available from <<http://crmht-europe.cnrs-orleans.fr>>.
- [19] J.A. Speers, G.V. Gibbs, *Am. Mineralogist* 61 (1976) 238.
- [20] G.A. Parks, *Chem. Rev.* 65 (1965) 177.
- [21] C. Serre, F. Taulelle, G. Ferey, *Chem. Commun.* (2003) 2755.
- [22] R.C.T. Slade, J.A. Knowles, D.J. Jones, J. Roziere, *Solid State Ionics* 96 (1997) 9.
- [23] L. Szirtes, L. Riess, J. Megyeri, *J. Therm. Anal. Calorimetry* 73 (2003) 209.
- [24] B.B. Sahu, K. Parida, *J. Coll. Interface Sci.* 248 (2002) 221.
- [25] G. Alberti, M.S. Whittingham, *Intercalation Chemistry*, Academic Press, New York, 1982.
- [26] C. Schmutz, P. Barboux, F. Ribot, F. Taulelle, et al., *J. Non Cryst. Solids* 170 (1994) 250.
- [27] A.M. Kalinkin, E.V. Kalinkina, V.N. Makarov, *Int. J. Miner. Process.* 69 (2003) 143.
- [28] P.L. Stanghellini, E. Boccaleri, E. Diana, et al., *Inorg. Chem.* 43 (2004) 5698.
- [29] A. Bortun, E. Jaimez, R. Llavona, et al., *Mater. Res. Bull.* 30 (1995) 413 and references therein.
- [30] S. Bruque, M.A.G. Aranda, E.R. Losilla, et al., *Inorg. Chem.* 34 (1995) 893.
- [31] A.M.K. Andersen, P. Norby, *Inorg. Chem.* 37 (1998) 4313.
- [32] H. Nakayama, T. Eguchi, N. Nakamura, et al., *J. Mater. Chem.* 7 (1997) 1063.
- [33] Y.J. Li, M.S. Whittingham, *Solid State Ionics* 63 (1993) 391.
- [34] A.M.K. Andersen, P. Norby, T. Vogt, *J. Solid State Chem.* 140 (1998) 266.
- [35] J.S. Hartman, R.L. Millard, E.R. Vance, *J. Mater. Sci.* 25 (1990) 2785.
- [36] M.R. Rowles, J.V. Hanna, K.J. Pike, M.E. Smith, B.H. O'Connor, *Appl. Magn. Reson.* 32 (2007) 663.
- [37] K.J.D. Mackenzie, M.E. Smith, *Multinuclear Solid-State NMR of Inorganic Materials*, Pergamon, Amsterdam, 2002.
- [38] E.R. Nightingale Jr., *J. Phys. Chem.* 63 (1959) 1381.
- [39] A.I. Bortun, L.N. Bortun, A. Clearfield, *Chem. Mater.* 9 (1997) 1854.
- [40] A.I. Bortun, L.N. Bortun, D.M. Poojary, O. Xiang, A. Clearfield, *Chem. Mater.* 12 (2000) 294.
- [41] L.M. Sharigin, M.L. Kalyagina, S.I. Borovkov, *Russ. J. Appl. Chem.* 78 (2005) 229.
- [42] M. Pozin, *Technology of Inorganic Fertilizers*, Khimia, Moscow, 1965, p. 432.